N-ГФИ–АИБН возрастает в 1,5 раза по сравнению с использованием одного АИБН.

Заключение

Доказана целесообразность использования *N*-гидроксифталимида и его структурных аналогов в качестве катализаторов в процессах жидкофазного окисления алкилароматических углеводородов. Обоснована возможность интенсификации процесса окисления ИПБ до гидропероксида с участием этих катализаторов без изменения технологии процесса, что позволит снизить себестоимость получения фенола и ацетона. Установлена возможность повторного использования *N*-ГФИ и его способность самостоятельно активировать процесс окисления без участия инициаторов и сокатализаторов.

Рассмотрен механизм реакции окисления алкилароматических углеводородов до гидропероксидов в присутствии *N*-гидроксифталимида. Найдено соотношение констант скорости отрыва атома водорода пероксирадикалом от молекулы *N*-ГФИ и углеводорода (k_f/k_2), показывающее, насколько быстрее протекает реакция продолжения цепи пероксирадикала с *N*-ГФИ, чем реакция с углеводородом.

Литература

1. *Ларин Л.В., Егорова Е.В., Ананьева Е.А.* // Вестник МИТХТ. 2008. Т. 3. № 3. С. 52.
2. *Лебедев Н.Н.* Химия и технология основного органического и нефтехимического синтеза. М.: Химия, 1988.
3. *Кошель Г.Н., Смирнова Е.В.* // Катализ в промышленности. 2010. № 3. С. 26.
4. Пат. 2186767 РФ, МПК[7] C07C409/10, C07C409/08. Способ получения гидропероксидов / Мацуи Сигеказу, Курода Хироси. 1998.
5. *Ishii Y., Sakaguchi S.* // Adv. Synth. Calal. 2001. V. 143. P. 395.
6. Константы скорости гомолитических жидкофазных реакций: Справочник / Е.Т. Денисов. М.: Наука, 1978. С. 712.
7. *Кошель Г.Н.* Исследования в области окислительных превращений циклических углеводородов и ряд синтезов на этой основе: Дис ... д-ра хим. наук. Ярославль, 1975.
8. *Amorati R., Lucarini M., Mugnaini V.* // J. Org. Chem. 2002. V. 5. P. 1747.
9. *Опейда И.А., Компанец М.А., Кущ О.В.* // Нефтехимия. 2009. Т. 49. № 5. С. 409.

UDK 544.47; 547.571

SYNTHESIS OF METAL INTERCALATED CLAY CATALYSTS FOR SELECTIVE HYDROGENATION REACTIONS

© 2012 г. **D. Manikandan**[1,3], **R.V. Mangalaraja**[1], **S. Ananthakumar**[2], **T. Sivakumar**[3]

[1] Advanced Ceramics and Nanotechnology Laboratory, Department of Materials Engineering, Faculty of Engineering, University of Concepcion, Concepcion, Chile

[2] Materials and Minerals Division, National Institute for Interdisciplinary Science and Technology (NIIST), CSIR, Trivandrum, India

[3] Catalysis Laboratory, Department of Chemical Engineering, A.C. College of Technology, Anna University, Chennai – 600 025, India

1. Introduction

Environmentally safe functional catalyst for organic reactions is an emerging field of «green chemistry». The nanotechnology guided design and synthesis of novel catalysts show enhanced performance in their catalytic activity or selectivity. Chemical industries engaged in synthetic organics especially design and synthesis of drug intermediates, natural products, bioethanol and oil extraction seriously looking for new molecular/catalyst

materials. Many nano catalysts show regenerative quality by thermal or chemical treatments for repeated use and it reduces the cost of the chemical synthesis. Economically, the nanostructured catalysts have societal benefits in their energy efficiency as well as by cutting the hazardous gaseous-emissions and minimizing the industrial water pollution [1]. Metal nano catalysts exhibit large surface areas have been found applications in wide range of chemical reactions including hydrogenation, hydrosilylation, hydrogenolysis, Heck-type coupling, oxidation reactions etc [2—5]. Zeolite type porous materials with pore size of subnanometers and clay minerals intercalated with transition metal ions having high surface area have been employed as catalysts very successfully even today for many industrial chemicals [6—9]. Swelling nature and ion exchange property of the clays are the important advantages in clay catalysts where one can exchange bulky organic cations easily during synthesis.

Supported noble metal catalysts with particle size down to a few nanometers are recommended in today's chemical processes. Importantly, deliberate tailoring of particle size, shape and surface could lead to improved or new catalytic properties. The generation of metal particles of nanometer size in the interlamellar space of the clay minerals was found to be a favorable technique for synthesizing well dispersed and stable metal catalysts. The use of such catalysts in selective hydrogenation reactions overcomes the disadvantages like poor metal reduction, less selectivity, side reactions like condensation and cyclisation met with the conventional porous and supported catalysts.

Heterogeneous catalysts used in hydrogenation reactions contain usually an active metal species supported on a carrier. The metal is able to adsorb hydrogen thus making hydrogenation reaction possible. The carrier is able to disperse the metal to smaller particles as compared to bulk metal enhancing the specific metal surface area. Additionally, smaller metal particles partially behave as non-metals, e.g. have higher electron densities, leading to higher hydrogenation rates compared to larger particles [10]. In addition to the electronic effects which vary from metals to metals, geometric dimensions of the metal particles also influence the kinetics of the hydrogenation reaction and selectivity if the size of the reacting molecule is close to the size of metal crystallites [11]. Activity and selectivity depend not only on the metal type and dispersion but also on the support. Secondly the electronic properties of the active metal can be modified by a promoter which in turn modifies the catalytic activity. In the preparation of supported catalyst, a high degree of dispersion of metal particles is important for maximizing the contact area of the catalyst with the reactant. It also minimizes the fraction of catalyst that is buried within the large particles which are unable to participate directly in the catalysed reaction. The mass transport in both reactants and reaction products is also increased when size of the catalyst particles are reduced to nanometer [12].

The main task of the support material is to carry the metal catalyst more homogeneously throughout the material. Supports can have different properties, like surface area ranging from 10 to 1200 m^2/g or even higher, pore volumes, pore diameter, surface acidities, electronic and geometric properties. Mostly, all conventional support materials are either acidic or basic oxides or different types of carbons. The mostly used support materials in chemoselective hydrogenation reactions are the bifunctional catalysts, exhibiting both acidic sites and an active metal, like metal containing zeolites [13—16] and mesoporous materials [15, 17—19], or metal impregnated/intercalated clays [20—23].

In general, it can be stated that oxide supports can provide stronger interactions with the main metal than carbon materials but the complete reduction of the metal is more difficult on the oxide compared to carbon [24]. Monometallic catalysts supported on Al_2O_3 and SiO_2 have produced very often saturated aldehydes as the main products in chemoselective hydrogenation of unsaturated aldehydes [25—27]. Acidic oxides are found to promote side reactions, for instance alumina favours cyclisation of cintronellal in citral hydrogenation [28] and formation of condensation products from furfural [29]. Basic supports can exhibit electron rich properties towards the active metal [30].

Traditionally approaches such as co-precipitation, deposition-precipitation, ion- exchange, impregnation,

Manikandan Dhanagopal *– Ph.D., Post Doctorate Researcher, Advanced Ceramics and Nanotechnology Laboratory, Department of Materials Engineering, Faculty of Engineering, University of Concepcion, Concepcion, Chile. Catalysis Laboratory, Department of Chemical Engineering, A.C. College of Technology, Anna University, Chennai – 600 025, India. Phone: 0056-41-2203664. E-mail: dmani_cat@yahoo.co.in*

Mangalaraja Ramalinga Viswanathan *– Ph.D., Associate Professor, Advanced Ceramics and Nanotechnology Laboratory, Department of Materials Engineering, Faculty of Engineering, University of Concepcion, Concepcion, Chile. Phone: 0056-41-2207389. E-mail: mangal@udec.cl*

Ananthakumar Solaiappan *– Ph.D., Scientist, Materials and Minerals Division, National Institute for Interdisciplinary Science and Technology (NIIST), CSIR, Trivandrum, India. Phone: 0091-471-2515289. E-mail: ananth777kumar@yahoo.com*

Sivakumar Thiripuranthagan *– Ph.D., Assistant Professor, Catalysis Laboratory, Department of Chemical Engineering, A.C. College of Technology, Anna University, Chennai – 600 025, India. Phone: 0091-44-944159636. E-mail: sivakumar@annauniv.edu*

successive reduction and calcination etc. were practiced to synthesize metal catalysts on support materials [31]. A disadvantage is however the lack of control over size, shape and stability of the produced nanoparticles. An ideal nanoparticle catalytic system should not only be catalytically accessible but also morphologically stable or controllable.

The interlayer space available in the clay minerals was found to be a very good nano phase reactor to host finely dispersed metal catalysts without aggregation [20, 22, 23]. In this work noble metal intercalated/impregnated clays have been attempted for a few selective organic synthesis reactions.

Hydrogenation of C=O bond alone is more difficult than C=C bond hydrogenation in α, β unsaturated aldehydes because the thermodynamic and kinetic data [32] favour the hydrogenation of only C=C bond. This decade long difficulty is to be solved in the area of fine chemical synthesis. In this context selective hydrogenation of cinnamaldehyde to cinnamyl alcohol has become one of the highly potential organic transformations in fragrance and flavour industries [33—37]. In general, acquiring maximum selectivity with high conversion is a tough task. This is because of various factors such as nature of the metal, nature of the support, method of synthesis, particle size of the metal catalysts, solvent, reaction temperature, hydrogen pressure etc. have individual influence in determining the activity and selectivity of the catalysts. The effect of all the above parameters on the conversion and selectivity in the selective hydrogenation of cinnamaldehyde has been reported in the review by Maki Arvela et al [10] and references therein. It is known that a properly designed catalyst should strongly polarize only the carbonyl group of the adsorbed aldehyde molecule for the adsorption and enhance its reactivity towards hydrogen. Hydrogenation of cinnamaldehyde was studied over different transition and noble metals supported on various conventional supports like metal oxides, mesoporous materials and smectite type clays [16, 38]. Among the various noble metal catalysts studied, platinum and ruthenium were found to produce more promising results towards the selective hydrogenation of cinnamaldehyde in liquid phase due to their larger d orbitals compared to Pd [39].

Here we presents the results obtained in the liquid phase hydrogenation of cinnamaldehyde over synthesised platinum or ruthenium intercalated montmorillonite/hectorite catalysts at different temperatures and hydrogen pressures. The effect of solvent and time on stream on the conversion and selectivity were studied and discussed. Comparison of catalytic activity of the intercalated hectorite catalysts and the impregnated catalysts was also made with respect to hydrogenation of cinnamaldehyde.

2. Experimental methods

2.1 Synthesis of metal intercalated clay catalysts

Known amount of montmorillonite was first ion exchanged by stirring with 2M NaCl solution to ensure that all the exchangeable cations are only Na^+. Dried Na-montmorillonite or Li-hectorite (3 g) as received from «Wako Pure Chemical Industries Ltd.» (Japan) were dispersed in 200 mL of water and allowed to swell separately for about 6 hours by continuous stirring. Surfactant assisted synthesis was employed for obtaining metal nano particulate sol. In a typical synthesis, platinum or ruthenium nanosol was

Table 1
Catalysts synthesized and their codes

Method	Clay	Metal	Wt.% (theoretical)	Catalyst Code
Intercalation	Montmorillonite	Platinum	1	Pt-CTA-MM1
			2	Pt-CTA-MM2
		Ruthenium	1	Ru-CTA-MM1
			2	Ru-CTA-MM1
	Hectorite	Platinum	1	Pt-CTA-Hec1
			2	Pt-CTA-Hec2
		Ruthenium	1	Ru-CTA-Hec1
			2	Ru-CTA-Hec2
Impregnation	Montmorillonite	Platinum	1	Pt-MM1
			2	Pt-MM2
		Ruthenium	1	Ru-MM1
			2	Ru-MM2
	Hectorite	Platinum	1	Pt-Hec1
			2	Pt-Hec2
		Ruthenium	1	Ru-Hec1
			2	Ru-Hec2

prepared by adding the metal precursors such as hexachloroplatinic acid or hexammineruthenium chloride containing 1 and 2 % w/w platinum or ruthenium respectively in water in presence of cetyltrimethylammonium bromide and stirred for 2 hours. Critical micelle concentration of surfactant (CMC) is the minimum concentration at which micelle is formed in an aqueous solution. The formation of micelle helps to prevent the metal particles from aggregation due to coalescence by forming a surface adlayer around the particles and stabilize the particles in a dispersed state in solution [40]. Well dispersed particles were obtained only when the concentration of the surfactant was 10 times of its CMC (CMC of CTAB is 0.92 mmol/Lit). Further increase in surfactant concentration resulted in precipitation. Therefore the concentration of surfactant was taken as 10 times its CMC in the synthesis of catalysts. The cationic surfactant also helped in the long-term stability of the metal hydrosol, since the vertically oriented [40] surfactant bilayer was adsorbed onto the surface of the metal nano particles (electrostatic and steric stabilization).

Then the precursor in the micelles was reduced to metallic state by dropwise addition of aqueous solution of $NaBH_4$ (0.05 g in 10 ml of distilled water) and stirred for about 3 hours. Black coloured metal nanosol was finally obtained which was added separately to the aqueous suspension of the corresponding clay and left under vigorous stirring for about 24 hours. The ion exchange reaction of Na^+ in the case of montmorillonite and Li^+ in the case of hectorite with cetyltrimethylammonium cation (CTA^+) resulted in the formation of organoclay complex with simultaneous intercalation of the Pt or Ru particles respectively into the internal clay surface (interlamellar) [41, 42]. The metal intercalated organo clay samples (black in colour) were washed thoroughly with ethanol and toluene to remove the excess surfactant in solution and air-dried. The different catalysts synthesized are listed in Table 1.

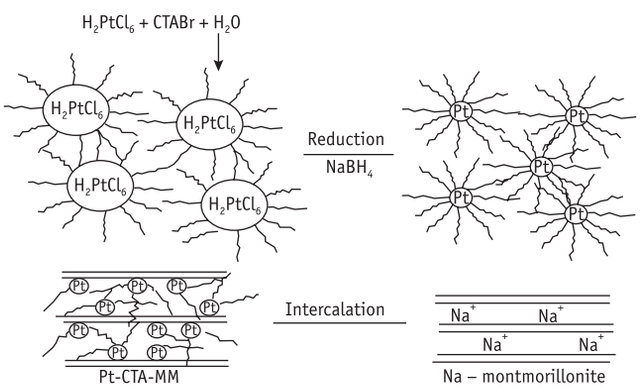

Fig. 1. Schematic representation of synthesis of Pt-CTA-MM

The ion exchanging property of the smectite clays was effectively utilized in this study for generating metal nano particles in the interlamellar space of the smectite clays. The reaction between Na^+ or Li^+ ions in the interlayer space and CTA^+ ions in micelle is the driving force for the intercalation of active metal nano particles into the interlamellar space. The CTA^+ ions involved in the ion exchange reaction with Na^+ ions rendered the clay surface hydrophobic. Schematic representation of synthesis of platinum intercalated montmorillonite catalysts is shown in Figure 1.

2.2 Synthesis of metal impregnated clay catalysts

Metal impregnated montmorillonite and hectorite catalysts were synthesised using wet impregnation technique. In a typical preparation, 1 g of montmorillonite or hectorite was first preheated at 350 °C for 3 hours to clean the pore surface. It was then dispersed into an aqueous solution containing required amount of corresponding metal precursor salt to get 1 and 2 % w/w metal impregnated samples. Then the mixture was refluxed for 3 hours under vigorous stirring for homogeneous mixing and allowed for evaporation of water in air oven at 110 °C. The dried catalysts were reduced in a slurry phase using aqueous solution of $NaBH_4$ and dried. The solid materials obtained were ground and labeled as shown in Table 1.

2.3 Physicochemical Characterization

All the synthesised catalysts were subjected to X-ray diffraction analysis in the region of $2\theta = 1.0°$ to 50° (Philips X'pert X-Ray Diffractometer using Cu—K_α radiation of wave length $\lambda = 1.54$ E). For the transmission microscopic analysis the intercalated catalysts were dispersed in isopropanol, drop of this dispersion was placed on a copper grid and TEM photographs were taken using JEOL JEM-2010F to determine the size of the noble metal particles. Few representative catalysts were subjected to elevated temperature before taking TEM micrographs to know effect of heat treatment on the metal particle size. Also the catalysts were characterized by atomic absorption spectrophotometric analysis (Perkin Elmer 2380). The specific surface area of representative samples were determined by BET method using nitrogen as an adsorbate with a Quantachrome Nova 4200 e surface area analyser. The samples taken in the sorption vessel were degassed at 150 °C under vacuum ($< 10^{-3}$ Torr) for 2 hours prior to adsorption measurements. TGA thermograms of the representative catalyst samples were studied in the temperature range of 50 to 600 °C at a heating rate of 20 °C/min by taking 10—15 mg of sample in an aluminum pan using Perkin Elmer

Diamond TG/DTA analyser. The chemical composition of clay minerals namely montmorillonite and hectorite used to synthesise metal intercalated/impregnated clay catalysts was determined by XRF analysis using X-ray fluorescence analyzer (Shimadzu EDX-8000). Catalyst samples (50 mg) were pelletized using a die and taken in the cell of XRF instrument for further determination.

2.4 Liquid phase hydrogenation

A high pressure SS hydrogenation reactor of capacity 150 ml provided with gas inlet and outlet valves, pressure gauge, thermocouple, stirrer and sampling vent was used for the entire study to check the performance of the catalyst synthesized. Prior to the start of the hydrogenation reaction, the catalyst (0.5 g) was activated at 373 K, 5 bar H_2 pressure for about 3 h in the presence of small amount of ethanol. After the activation, the reactor system was cooled down to room temperature and 0.02 mol of cinnamaldehyde was taken in the reactor along with the solvent (Ethanol) to bring the total volume of 75 ml for efficient stirring. The reactor was pressurized to 2 bar hydrogen pressure and depressurized after few minutes. This cycle of pressurization and depressurization was carried out at least three to four times to completely replace the air inside the vessel with hydrogen. Then the reactor was pressurized to 3 bar hydrogen pressure and reaction was performed for the duration of 5 h. Samples were withdrawn from the reactor periodically after every 1 h and the catalysate was subjected to gas chromatographic analysis (Shimadzu 17 A Gas Chromatograph fitted with OV 1 column and using FID detector). Representative samples were also analyzed by GCMS technique for the confirmation of the reaction products.

3. Results and discussions

3.1 UV-Visible spectrophotometric analysis

The UV-Visible spectrum of the colloidal Pt sol is shown in Figure 2. Before reduction the absorption peak appeared at $\lambda = 260$ nm due to $[PtCl_6]^{2-}$ ions [43]. But after reduction with $NaBH_4$, this absorption band disappeared and a new peak in the visible region ($\lambda = 502$ nm) was observed which indicated the complete reduction of precursor salt to zero valent platinum. The appearance of new peak at $\lambda = 502$ nm is due to the surface plasmon absorption which may be due to the regularity of the particle size in nm range [44].

3.2 X-ray diffraction analysis

X-ray diffraction patterns of Na-montmorillonite and Pt intercalated montmorillonite (Pt-CTA-MM 1 and Pt-CTA-MM 2) are shown in Figure 3. The d (001) reflection of Na-montmorillonite appeared at $2\theta = 6.1°$ corresponds to the d spacing value of 15 E and this 2 θ value shifted to $2\theta = 1.5°$ for the CTA^+ exchanged Pt montmorillonite catalysts which corresponds to d spacing of 59 E. The remarkable increase in the d spacing value of 59 E after the intercalation of CTA^+ cation in the interlayer space indicates the better swelling ability of the montmorillonite due to its higher CEC value among the other candidates in the smectite family. A small peak at 2 theta = 40° indicates the presence of nano crystalline platinum metal phases and the intensity of this peak increased when the percentage loading of platinum was increased (Fig. 3, *b, c*). Further, no shift in any other peak indicated the exchange of Na^+ with CTA^+ along with the incorporation of Pt metals in the interlayer surface did not alter the basic lattice structure of montmorillonite.

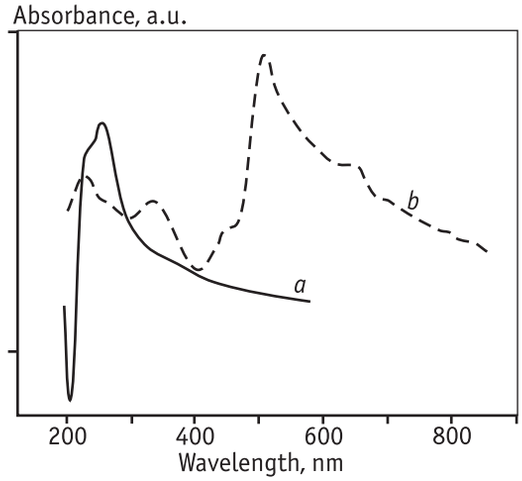

Fig. 2. UV-Visible absorption spectra of hexachloroplatinic acid before reduction (*a*) and after reduction (*b*)

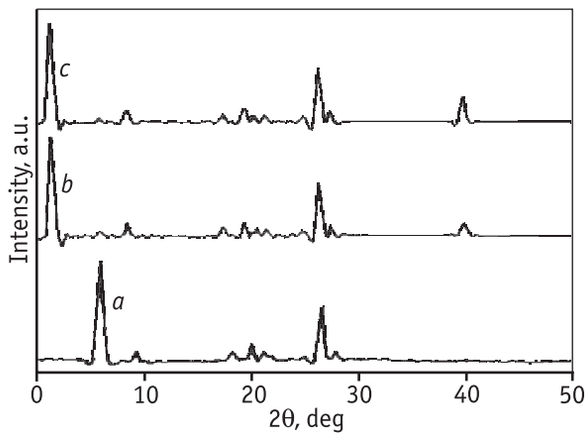

Fig. 3. X-ray diffraction patterns of Na-MM (*a*), Pt-CTA-MM 1 (*b*) and Pt-CTA-MM 2 (*c*)

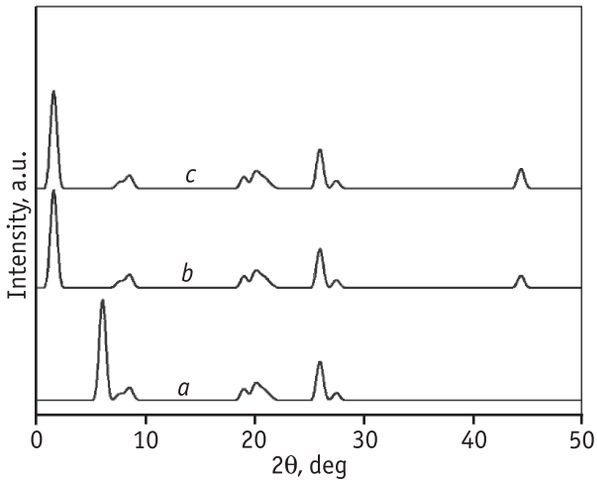

Fig. 4. X-ray diffraction patterns of Na-MM (*a*), Ru-CTA-MM 1 (*b*) and Ru-CTA-MM 2 (c)

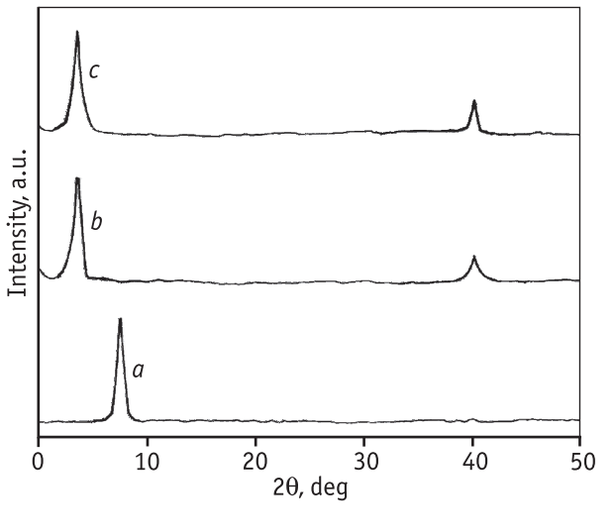

Fig. 5. X-ray diffraction patterns of Li-Hec (*a*), Pt-CTA-Hec 1 (*b*) and Pt-CTA-Hec 2 (c)

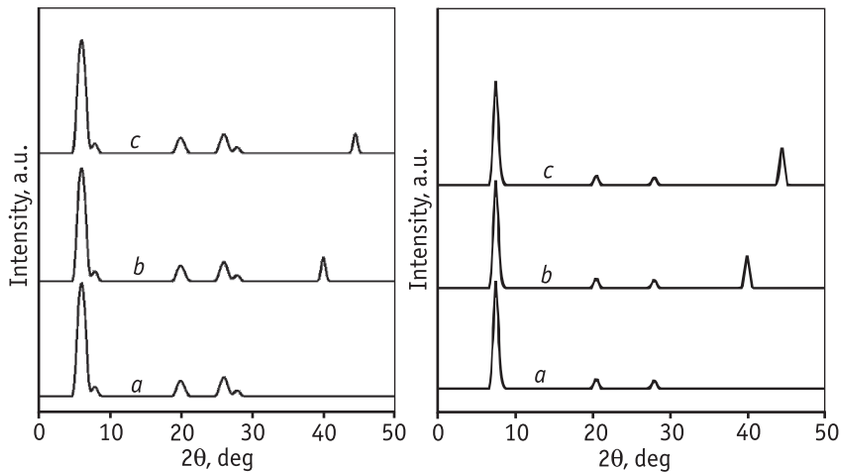

Fig. 6. X-ray diffraction patterns of Na-MM (*a*), Pt-MM 2 (*b*) and Ru-MM 2 (c) (left); Li-Hec (*a*), Pt-Hec 2 (*b*) and Ru-Hec 2 (c) (right)

The ruthenium intercalated montmorillonite catalysts also show similar XRD patterns (Fig. 4) as that of platinum intercalated montmorillonite catalysts. A shift from $2\theta = 6.1^\circ$ (*d* spacing 15 E) to $2\theta = 1.5^\circ$ (*d* spacing 59 E) and the (111) peak observed at $2\theta = 44.5^\circ$ confirmed the presence of ruthenium in the intercalated montmorillonite catalysts.

The XRD patterns of Li-hectorite is shown in Figure 5,*a* in which the first order reflection appeared at $2\theta = 7.4^\circ$ (12 E). The same peak after the modification with cationic surfactant (CTAB) was shifted to $2\theta = 4.6^\circ$ (19 E). The shift in 2θ value of *d* (001) reflection to lower side revealed that the basal spacing increased due to the incorporation of bigger organic moiety in the interlamellar space by replacing Li^+. The increase in basal spacing in hectorite was less when compared to montmorillonite. This is because of the lower CEC value of hectorite compared to montmorillonite. The CEC value (87 meq/100 g, 49 meq/100 g for montmorillonite and hectorite respectively) determines the amount of intake of surfactant cation (CTA^+), which in turn causes the increase in basal spacing. Greater the exchange of bulky organic cation greater is the basal spacing. The lattice structure of the clay minerals was not affected much during the introduction of metal particles along with the surfactant micelle.

XRD patterns of the metal impregnated clay catalysts are shown in Figure 6. No significant swelling was observed for metal impregnated clay catalysts and therefore there was no shift in (001) peak in the XRD patterns. It is clear from the XRD patterns that impregnation of noble metals does not alter the lattice structure of clay minerals.

3.3 Transmission electron microscopic analysis

Transmission electron microscopic images of platinum intercalated and ruthenium intercalated montmorillonite catalysts (Pt-CTA-MM1, Pt-CTA-MM2, Ru-CTA-MM 1, Ru-CTA-MM 2) are shown in Figure 7. Fair and uniform dispersion was obtained with almost all the catalysts. The average diameter of the particles was calculated and reported in Table 2. The diameter of the particles was in nm range confirming the effect of CTAB surfactant. The presence of surfactant cations in the interlamellar space swell the layer spacing so that the particles have a greater chance to disperse over a wide space.

Table 2
Physico-chemical properties of montmorillonite catalysts

Materials	Metal content[a], wt. %	a^{S}_{BET}, m^2/g	$2\theta^b$, deg		d spacing, Å	d^c_{ave}, nm
			$d(001)$	(111)		
Na-Mont	–	209	6.0	–	15	–
CTAM	–	91	1.5	–	59	–
Pt-CTA-MM 1	0.98	129	1.5	40	59	2.7
Pt-CTA-MM 2	1.97	–	1.5	40	59	6.9
Ru-CTA-MM 1	0.89	113	1.5	44.5	59	11.2
Ru-CTA-MM 2	1.98	–	1.5	44.5	59	21.7

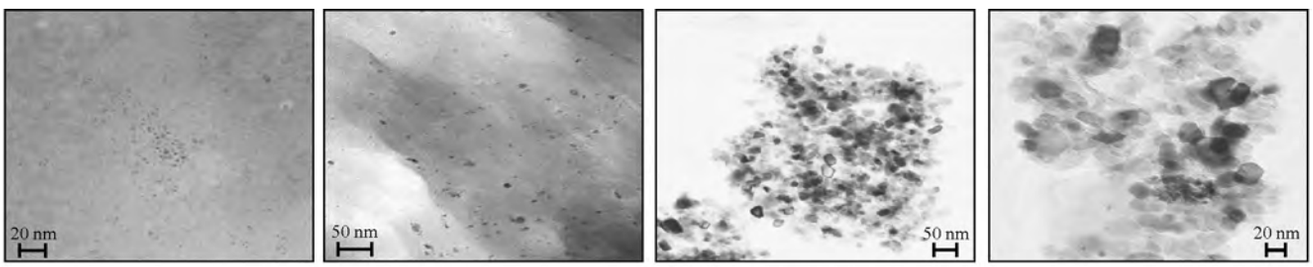

Fig. 7. TEM micrograph of Pt-CTA-MM 1, Pt-CTA-MM 2, Ru-CTA-MM 1, Ru-CTA-MM 2

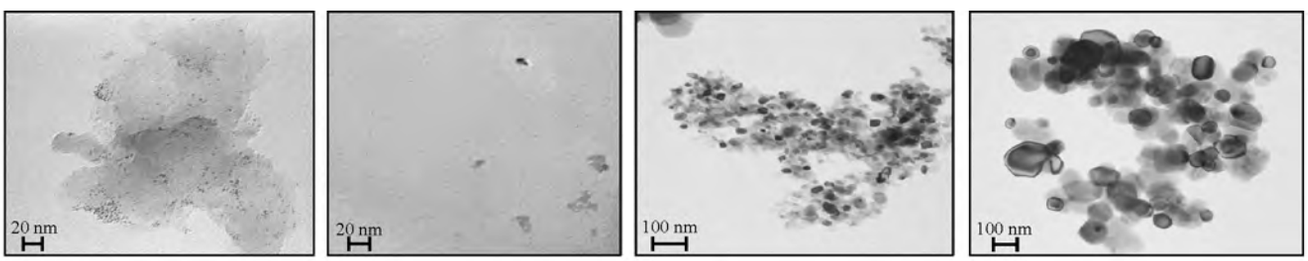

Fig. 8. TEM micrograph of Pt-CTA-Hec 1, Pt-CTA-Hec 2, Ru-CTA-Hec 1, Ru-CTA-Hec 2

The transmission electron micrographs of platinum intercalated hectorite catalysts (Pt-CTA-Hec 1, Pt-CTA-Hec 2) shown in Figure 8 indicate that the particle sizes are similar to that of Pt intercalated montmorillonite catalysts but the dispersion of particles is poor when compared to Pt-CTA-MM catalysts. TEM images observed on Ru-CTA-Hec 1, Ru-CTA-Hec 2 show that the particle size of Ru is greater in Ru-hectorite catalysts than in Ru-montmorillonite catalysts. This increase in particle size in these catalysts may be due to poor swelling of hectorite compared to montmorillonite.

The TEM images of some of the representative catalysts subjected to high temperature treatment (400 °C) are shown in Figure 9. From the pictures, it is clear that when catalysts were subjected to elevated temperatures, due to the decomposition of surfactant, aggregation of particles occurred leading to the formation of bigger particles which process is commonly referred as coalescence [24].

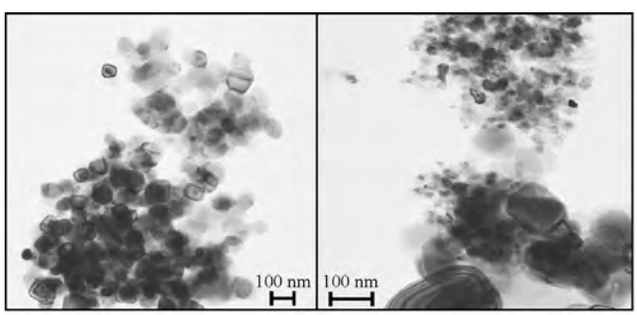

Fig. 9. TEM micrograph of Pt-CTA-MM 1, Ru-CTA-MM 1 pretreated at 400 °C

Table 3
Physico-chemical properties of hectorite catalysts

Materials	Metal content[a], wt. %	a^{S}_{BET}, m^2/g	$2\theta^{b}$, deg		d spacing, Å	d^{c}_{ave}, nm
			$d(001)$	(111)		
Li-Hec	–	47	7.4	–	12	–
CTA-Hec	–	34	4.6	–	19	–
Pt-CTA-Hec 1	0.92	41	4.6	40	19	2.3
Pt-CTA- Hec 2	1.68	–	4.6	40	19	9.5
Ru-CTA- Hec 1	0.93	42	4.6	44.5	19	21.3
Ru-CTA- Hec 2	1.85	–	4.6	44.5	19	24.5

3.4 BET surface area analysis

The surface areas of the different smectite clay minerals used as support materials are given in Tables 2 and 3. Clay minerals are generally used as catalysts and support materials to disperse the metals or metal complexes because of the tunable acidic behaviour and interlayer space. The surface area of the clay minerals in turn depends on the space available between the silicate layers. As montmorillonite is one of the major candidates of the smectite group of clay minerals with larger interlayer space, its surface area is higher when compared to other members studied in the same smectite family (Na-MM = 209 m^2/g, Li-Hec = = 47 m^2/g). But in all the cases the surface area decreased when they were intercalated with bulky surfactant cations (CTAM = 91 m^2/g, CTA-Hec = 34 m^2/g). The decrease in surface area of the surfactant exchanged clay materials may be attributed to exchange sites which were satisfied by CTA with large molecular size resulting in inaccessibility of the internal surface to the nitrogen gas and blocking of the micropores in the surfactant modified clays. The major increase in surface area of the surfactant stabilized metal intercalated catalysts (Pt-CTA-MM 1 = 129 m^2/g, Ru-CTA-MM 1= 113 m^2/g, Pt-CTA-Hec 1= 41 m^2/g and Pt-CTA-Hec 2 = 42 m^2/g) is due to the fact that, during the intercalation of surfactant stabilized metal sol the interlamellar space of the clay material may significantly expanded (because of the vertical orientation of surfactant bilayer onto the surface of the metal nanoparticles) which inturn increases its surface area. This increase in surface area is also added with the contribution from the metal particles.

3.5 Atomic absorption spectrophotometric analysis

AAS analysis of the catalysts samples clearly shows the presence of actual metal contents in the clay minerals. The results reported in Tables 2 and 3 indicate the concentrations of the metals in the catalysts. One can notice that they are almost equal to the calculated amounts taken during the preparation of catalysts.

3.6 Thermo gravimetric analysis

The thermogram of Na-montmorillonite and Li-hectorite and their corresponding surfactant modified forms are shown in Figure 10. The thermogram indicates that there are two stages of weight losses. The first one around 90 °C was assigned for the loss of adsorbed water molecules. The second loss between 170 °C and 350 °C was due to the decomposition of surfactant ions.

The TGA reports reveal that the catalysts can be subjected to maximum temperature of 270 °C, beyond which the decomposition of surfactant leads to the formation of metal cluster with increased diameter. The TEM pictures taken for the catalysts heat treated at 400 °C have confirmed the increase in particle size. From the TGA analysis, one could understand the thermal stability and service temperature range during the synthesis of industrial chemicals.

3.7 X-ray fluorescence analysis

X-Ray fluorescence analysis was carried out to determine the chemical composition of the clay minerals. Table 4 shows the percentage composition of various elements in montmorillonite and hectorite clays in their oxide form.

4. Hydrogenation of cinnamaldehyde

4.1 Effect of temperature

The general reaction scheme of hydrogenation of cinnamaldehyde is shown in Figure 11. The effect of temperature at 3 bar hydrogen pressure on the conversion of

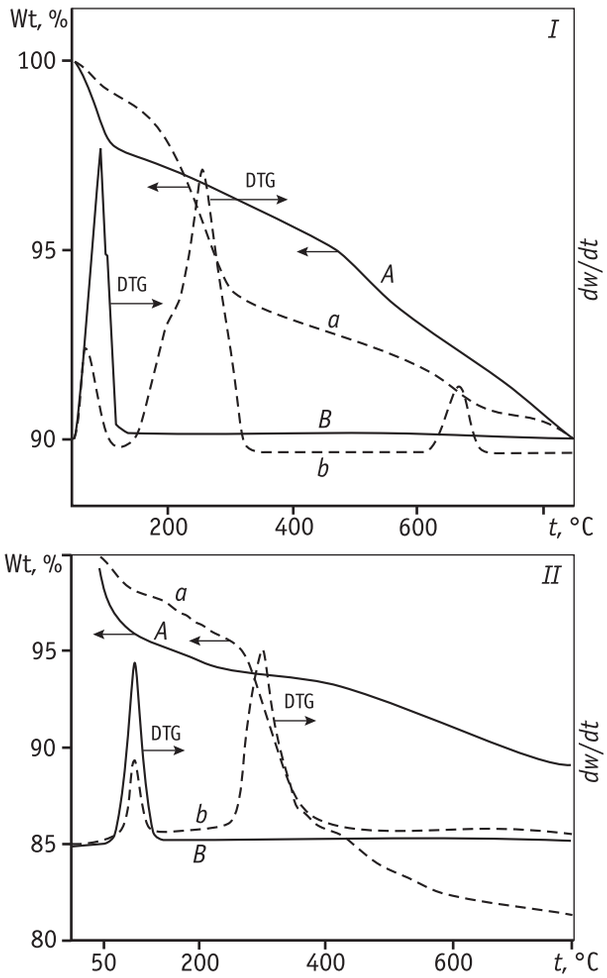

Fig. 10. TG thermogram of Na-MM (*A*) and CTA-MM (*a*), DTG thermogram of Na-MM (*B*) and CTA-MM (*b*) (*I*); TG thermogram of Li-Hec (*A*) and CTA-Hec (*a*), DTG thermogram of Li-Hec (*B*) and CTA-Hec (*b*) (*II*)

Table 4

Chemical composition of Na-Montmorillonite and Li-Hectorite

Name of the clay mineral / Chemical Constituents	Na-montmorillonite, (%)	Li-hectorite, %
Al_2O_3	66.2	–
SiO_2	17.1	61.7
MgO	1.8	29.5
CaO	1.5	–
H_2O	6.3	–
Na_2O	3.9	5.9
Li_2O	–	2.9
Others	3.2	–

cinnamaldehyde and selectivity towards cinnamyl alcohol over different amounts of platinum intercalated montmorillonite catalyst (Pt-CTA-MM 1) (viz. 0.1, 0.3 and 0.5 g) is depicted in Figure 12. At room temperature it was ob-

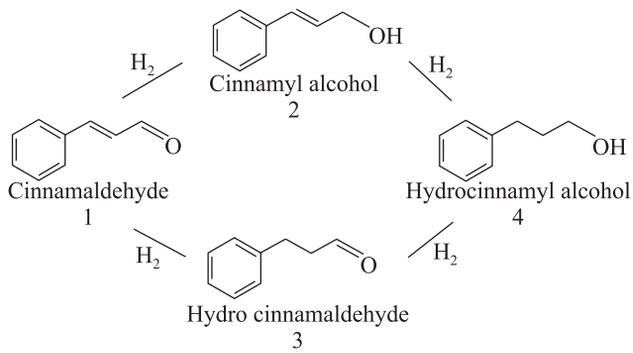

Fig. 11. Reaction scheme of hydrogenation of Cinnamaldehyde

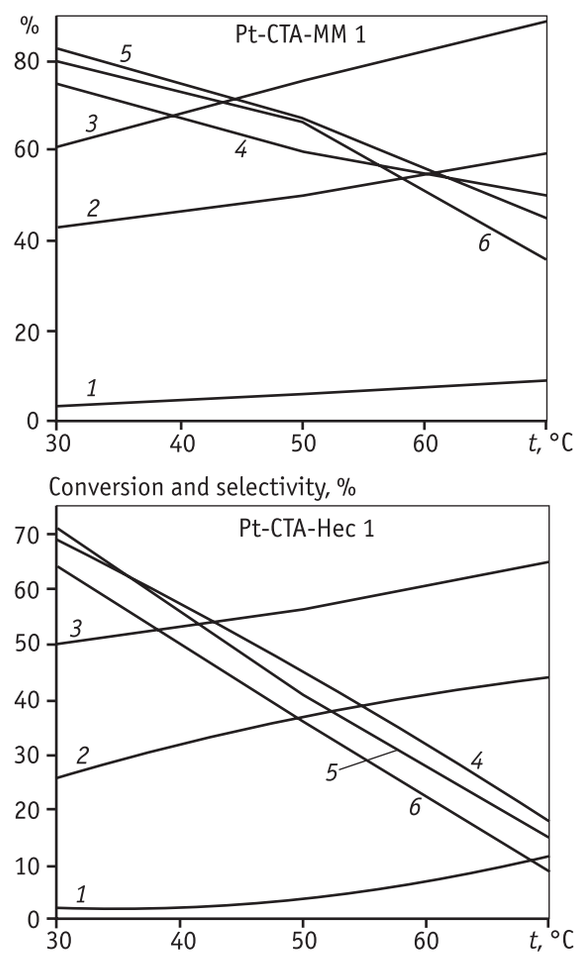

Fig. 12. Effect of temperature on the conversion of cinnamaldehyde and selectivity towards cinnamyl alcohol

1 – conv with 0.1 g; *2* – conv with 0.3 g; *3* – conv with 0.5 g; *4* – sel of COL with 0.1 g; *5* – sel of COL with 0.3 g; *6* – sel of COL with 0.5 g

served that 60 % conversion was obtained at the end of five hours and as the temperature increased the conversion increased linearly and reached a maximum of 89 % at 70 °C over 0.5 g of Pt-CTA-MM 1 catalyst. The increase in conversion with increase in temperature is due to the adsorption of more amounts of reactant molecule over the catalytic sites at higher temperature.

The selectivity of cinnamyl alcohol was also dependent on the reaction temperature. Low temperature favoured the formation of cinnamyl alcohol through the selective hydrogenation of C=O bond and the selectivity of cinnamyl alcohol decreased with the increase in temperature because of the competitive adsorption between cinnamaldehyde and the product cinnamyl alcohol simultaneously over more active catalytic sites. The product cinnamyl alcohol formed has sufficient energy to get adsorbed on the surface at higher temperature, which leads to further hydrogenation and thus decreasing the selectivity.

Hydrogenation of cinnamaldehyde was carried out with Pt-CTA-Hec 1 at different temperatures to study the effect of reaction temperature on the conversion level of cinnamaldehyde and selectivity towards cinnamyl alcohol and the results are plotted in Figure 12. The catalytic activity of Pt-CTA-Hec 1 at room temperature was compared with that of Pt-CTA-MM 1. The conversion and selectivity were found to be 50 and 64 % respectively over Pt-CTA-Hec 1 catalyst whereas Pt-CTA-MM 1 catalyst showed the conversion and selectivity of 61 and 80 % respectively. Figure 13 shows the histograms of conversion and selectivity of Ru-CTA-MM 1, Ru-CTA-MM 2, Ru-CTA-Hec 1 and Ru-CTA-Hec 2 catalysts at room temperature and at 9 bar hydrogen pressure for the reaction time of 5 hours. Among all the catalysts studied, Ru-CTA-MM 2 showed maximum conversion of 65 %.

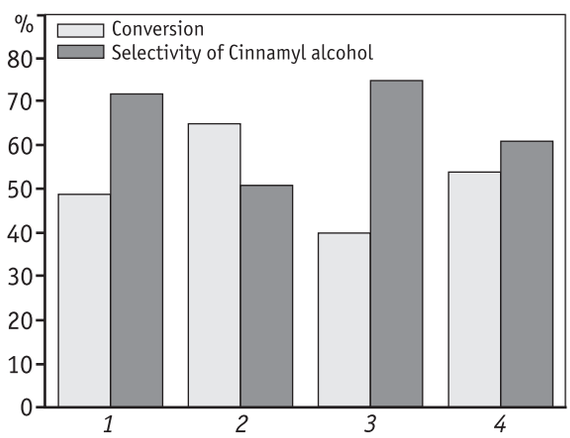

Fig. 13. Conversion of cinnamaldehyde and selectivity towards cinnamyl alcohol over Ru-CTA-MM 1 (*1*), Ru-CTA-MM 2 (*2*), Ru-CTA-Hec 1 (*3*) and Ru-CTA-Hec 2 (*4*)

Low conversion and selectivity over Pt-CTA-Hec 1 and Ru-CTA-Hec catalysts compared to Pt-CTA-MM 1 catalyst may be attributed to the less swelling ability which retards the diffusion of the reactant into the interlamellar space, lower acidity of hectorite compared to montmorillonite and may also be due to larger particle size in Pt-CTA-Hec catalysts. The fine dispersion and smaller particle size of Pt in Pt-CTA-MM 1 lead to the increase in the number of active sites and therefore the substrate has more chance of getting adsorbed on the catalyst. The higher conversion of Ru-CTA-MM 2 is due to the high concentration of metallic sites with very fine dispersion as montmorillonite offers greater interlayer spacing. But the selectivity towards cinnamyl alcohol over Ru-CTA-MM 2 was found to be less due to the greater size of the Ru particles.

The conversion and selectivity over Ru-CTA-MM 2 was found to be less than Pt-CTA-MM 2 at room temperature and at 9 bar hydrogen pressure. This difference in selectivity is due to the specificity of the metal in selectively hydrogenating the C=O or C=C bond in the hydrogenation of cinnamaldehyde [45]. The less selectivity of Ru catalysts may also be due to the fact that d orbital of Ru expands to a smaller extent [46], which results in the preferential adsorption of C=C bond over the catalytic sites because of less four electron repulsion compared to Pt catalysts. This is similar to the observation made by Giroir-Fendler et al [47].

4.2 Effect of pressure

The effect of hydrogen pressure on conversion and selectivity was also studied by varying the pressure of H_2 at room temperature (Fig. 14). The change in pressure of hydrogen affects the conversion level of cinnamaldehyde significantly. The conversion was directly proportional to the hydrogen pressure as observed by Satagopan and Chandalia [48] and Zhang et al [49]. From Figure 14, it is clear that the conversion increased as the hydrogen pressure increased from 3 bar to 9 bar and reached a maximum of 80 % over Pt-CTA-MM 1 at room temperature. Figure 14 also illustrates the effect of pressure of hydrogen on the conversion and selectivity of cinnamyl alcohol over Pt-CTA-Hec 1. As the hydrogen pressure of the reaction increased to 9 bar the conversion level increased to 73 %. This increase in the conversion with pressure is due to the availability of more amount of molecular hydrogen for adsorption on the metal sites. However the increase in hydrogen pressure did not influence the selectivity towards cinnamyl alcohol and the selectivity remained at 80 % in case of Pt-CTA-MM 1 at all the pressures.

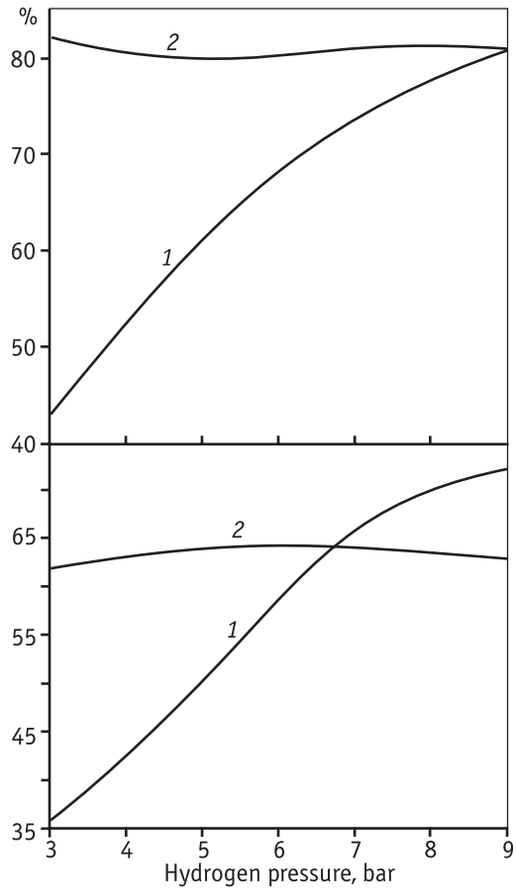

Fig. 14. Effect of hydrogen pressure on the conversion of cinnamaldehyde and selectivity towards cinnamyl alcohol
1 – conversion; *2* – selectivity

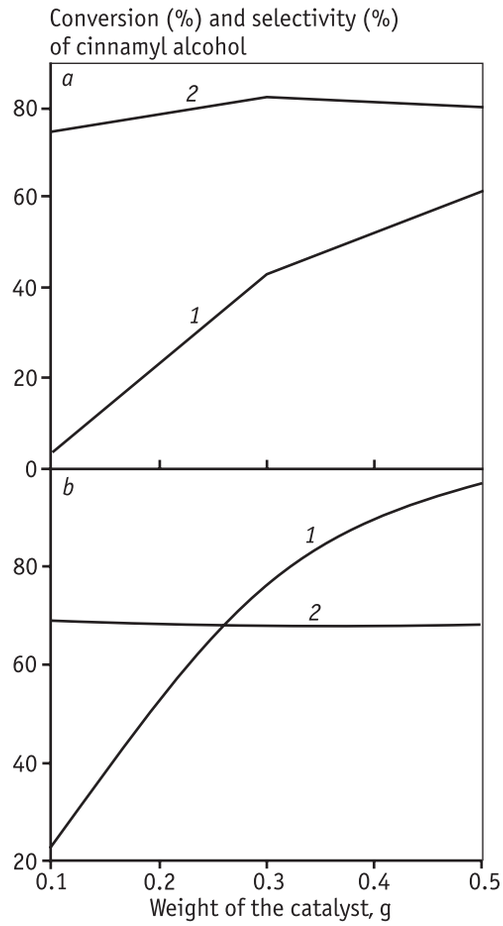

Fig. 15. Effect of weight of the catalyst on conversion of cinnamaldehyde and selectivity towards cinnamyl alcohol over Pt-CTA-MM 1 (*a*), Pt-CTA-MM 2 (*b*)
1 – conversion; *2* – selectivity

4.3 Effect of weight of the catalyst

Figures 15 show the effect of weight of intercalated montmorillonite catalyst on the conversion and selectivity. It was found that conversion of cinnamaldehyde increased with weight of the catalyst. This is because of the increase in number of active sites available for the substrate molecules. But the increase in weight of the catalyst has no effect on selectivity towards cinnamyl alcohol and in all the cases the selectivity towards cinnamyl alcohol remained the same as 78 and 65 % over Pt-CTA-MM 1 and Pt-CTA-MM 2 catalysts respectively.

4.4 Effect of time on stream on conversion

The effect of time on stream on conversion was studied and the results are shown in Figure 16. The reaction was carried out for 5 hours and the samples were withdrawn for every one hour interval and subjected to GC analysis. Reaction was almost absent with 0.1 g of the catalyst but with increase in weight of the catalyst the conversion increased linearly with time and found to be maximum (89 %) at the end of 5th hour with 0.5 g of catalyst. The results suggest that the conversion may increase further with the reaction time.

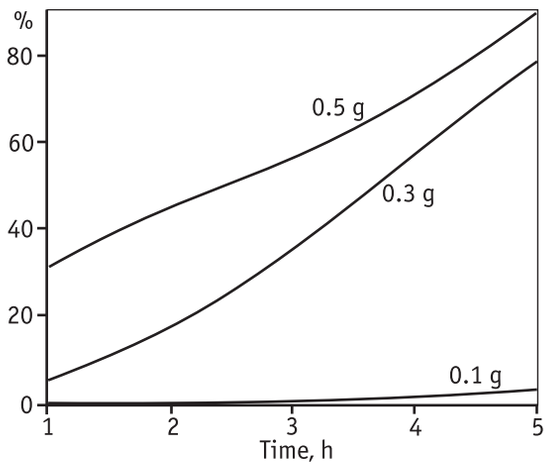

Fig. 16. Effect of time on stream on the conversion of cinnamaldehyde over Pt-CTA-MM1

4.5 Effect of solvent

The most important aspects in the liquid phase hydrogenation of α, β unsaturated aldehydes are solvent polarity, hydrogen solubility, interaction between the catalysts and the solvent [50] as well as solvation of reactants in the bulk liquid phase. Solvent effect in heterogeneous catalysed reactions on the catalytic activity has been reviewed by Singh and Vannice [51]. Hajek et al [52] studied the solvent effect on the hydrogenation of cinnamaldehyde over Ru/Y zeolite catalyst. The solvent used in the reaction played a major role in determining the selectivity of the desired product.

Therefore in the present study, hydrogenation reaction was carried out with three different solvents namely ethanol, isopropyl alcohol and *n*-hexane over Pt-CTA-MM 1 at 30 °C and 9 bar hydrogen pressure. The polarity of the solvent significantly influenced both conversion of cinnamaldehyde and selectivity towards cinnamyl alcohol.

The interaction between the solvent-solute and solvent-catalyst played a vital role in the catalytic performance. Reactions carried out in polar solvents (alcohols) exhibited high conversion and moderate selectivity whereas in the non polar medium, very poor conversion with high selectivity was observed (Fig. 17). Stronger hydrogen bonding between lone pair electrons of C=O group and OH group of alcohol may slightly prevent the hydrogenation of C=O bond when compared to C=C hydrogenation. Hydrogenation reaction in non-polar solvent such as *n*-hexane resulted in very low conversion of cinnamaldehyde but high selectivity towards cinnamyl alcohol. The more solubility of both hydrogen and the substrate molecule namely cinnamaldehyde in polar solvents leads to the higher conversion of cinnamaldehyde in the polar solvents [45].

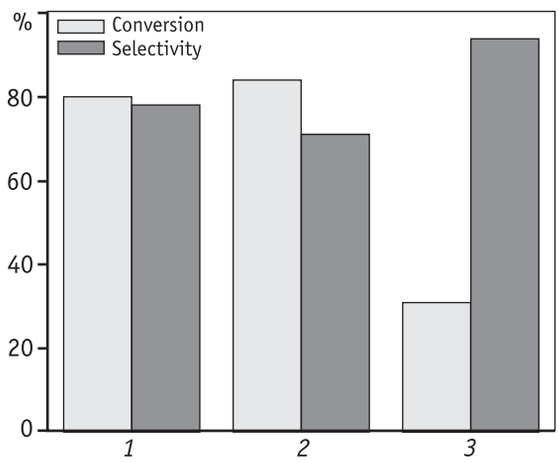

Fig. 17. Effect of solvent on the conversion of cinnamaldehyde and selectivity towards cinnamyl alcohol Ethanol (*1*), Isopropyl alcohol (*2*) and *n*-hexane over Pt-CTA-MM 1 catalyst (*3*)

4.6 Hydrogenation of cinnamaldehyde over impregnated platinum and ruthenium catalysts

Hydrogenation of cinnamaldehyde was also carried out over Pt and Ru impregnated montmorillonite, hectorite catalysts (Pt-MM 1, Pt-Hec 1, Ru-MM 1 and Ru-Hec 1) and the results are compared with that of intercalated catalysts. To study the effect of method of synthesis of catalysts on the catalytic activity, the obtained results with the metal intercalated and impregnated catalysts were compared. Figure 18 shows the conversion and selectivity towards cinnamyl alcohol at room temperature and at 9 bar pressure over different catalysts prepared by impregnation method. The results clearly show that the impregnated catalysts are not as good as intercalated catalysts as far as

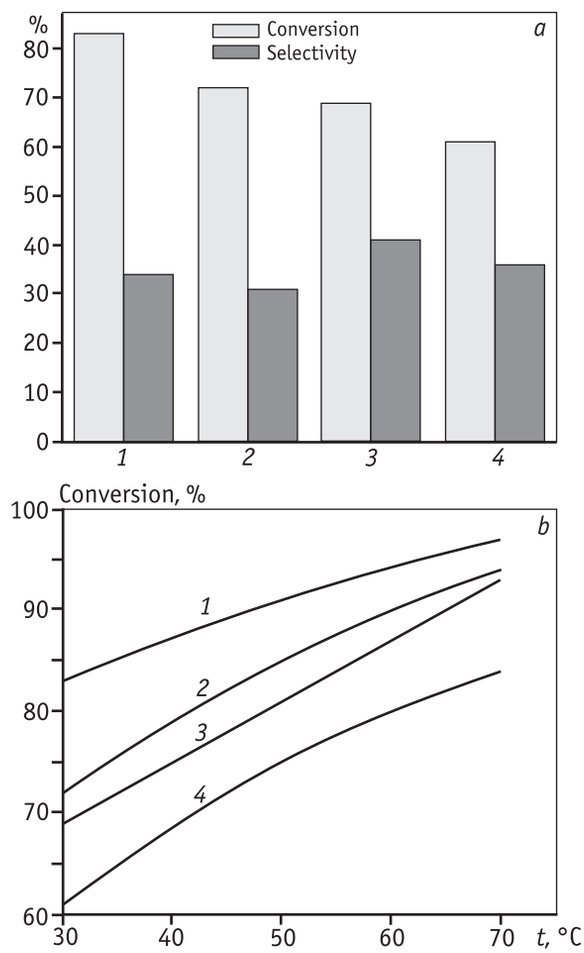

Fig. 18. Conversion of cinnamaldehyde and selectivity towards cinnamyl alcohol over Pt-MM 1 (*1*), Pt-Hec 1 (*2*), Ru-MM1 (*3*) and Ru-Hec 1 (*4*) (*a*); Effect of temperature on conversion of cinnamaldehyde over Pt-MM 1 (*1*), Pt-Hec 1 (*2*), Ru-MM1 (*3*) and Ru-Hec 1 (*4*) (*b*)

selectivity is concerned. Less selectivity may be due to the bigger particle size of the metal particles because of poor dispersion. Although 82 and 70 % conversion could be obtained over Pt-MM 1 and Ru-MM 1 catalysts, very poor selectivity was obtained over these catalysts. Similar observation was made also with hectorite catalysts irrespective of the metal species.

Figure 18 shows the effect of temperature on conversion of cinnamaldehyde over Pt-MM 1, Pt-Hec 1, Ru-MM 1 and Ru-Hec 1 catalysts. As the surface of impregnated catalyst is highly populated with metal particles, the increase in temperature increases the surface energy of these metallic sites favouring the easy adsorption of cinnamaldehyde molecule and also the transfer of hydrogen. The increase in temperature greatly influenced the hydrogenation rate in such a way that even 95 % conversion was obtained over Pt-MM 2 catalyst at 70 °C. As far as the selectivity was concerned the increase in temperature decreased the selectivity towards cinnamyl alcohol. This is because the more energetic catalytic sites favour consecutive hydrogenation through the adsorption of C=C bond of cinnamyl alcohol formed leading to hydro cinnamyl alcohol. As the size of metal particles in the impregnated catalysts were found to be greater than the catalysts obtained by the intercalation method, the orientation of reactant molecule may be different facilitating the C=C hydrogenation.

5. Conclusion

Intercalation of Pt and Ru metal nano catalysts into the clay minerals by the micellar technique is attempted. The technique is found to be attractive to homogeneously disperse metal catalysts within the interlamellar region of clay materials that can perform as nano reactors for synthetic organic molecules. XRD patterns confirm that the crystallinity of clay minerals was unaffected after the intercalation of metal nanoparticles. d spacing values obtained from X-ray diffraction patterns prove that montmorillonite swells to a larger extent (from 14.72 E to 59.23 E) when compared to hectorite (from 11.93 E to 19.2 E). TEM micrographs of metal intercalated and impregnated catalysts confirm the good dispersion of the Pt, Ru nanoparticles. Due to higher swelling capacity of montmorillonite than hectorite, better dispersion of metal particles was seen on the former than in the later. The diameter of the particles was found to be between 1—25 nm for the different catalysts synthesized. The thermogram of the organo clay evidenced that there are two stages of weight loss i.e. at 90 °C due to the loss of adsorbed water molecules and between 170 and 350 °C due to the decomposition of surfactant ions. This indirectly shows the thermal stability and temperature range for carrying out the catalytic reactions using metal intercalated catalysts. BET surface area analysis of the synthesised clay catalysts shows that the surface area values are good enough for carrying out catalytic hydrogenation reactions.

The results obtained in liquid phase hydrogenation of cinnamaldehyde over the synthesised catalysts indicate that all the catalysts could effectively be used as alternative catalysts for many other hydrogenation reactions. As far as hydrogenation of cinnamaldehyde is concerned, Pt-CTA-MM 1 catalyst was found to be the best catalyst which showed the maximum conversion of 60 % and selectivity of 79 % towards cinnamyl alcohol at room temperature and at 9 bar hydrogen pressure. Pt-CTA-MM 2 catalyst also showed higher conversion than Pt-CTA-MM 1 catalyst but the selectivity was comparatively less due to the presence comparatively larger size particles. The increased catalytic activity of Pt loaded montmorillonite catalysts with better selectivity is due to larger *d*-orbital expansion of Pt compared to Ru, larger interlayer spacing and more acidity of montmorillonite compared to hectorite. A hydrogen pressure of 9 bar and a reaction temperature of 30 °C respectively was optimized for achieving high conversion and selectivity. Increase in temperature and pressure only increased the conversion. The selectivity decreased with temperature and no significant change was observed with increase in pressure. Study of solvent effect in cinnamaldehyde hydrogenation reveals that polar solvent is better for significant conversion with maximum selectivity. Time on stream study revealed that there was no inhibition period for all the catalysts for all the reactions. Comparison of catalytic activity of Pt and Ru intercalated catalysts with Pt and Ru impregnated catalysts indicated that the intercalated catalysts were more selective towards the desired products namely cinnamyl alcohol. The impregnated catalysts showed more activity but less selectivity.

The authors would like to thank FONDECYT projects 3100010 (Postdoctorado) and 1100349, Government of Chile, Santiago.

References

1. C.M.P. Cientifica, Nano Catalysis and the Energy markets. 2002. Madrid, Spain.
2. *Liu Z., Wang C., Liu Z., Lu J.* // Appl. Catal. A: Gen. 344 (2008) 114.
3. *Ying B., Jiajian P., Yingqian H., Jiayun L., Huayu Q., Guoqiao L.* // Chinese Journal of Chemical Engineering, 17(6) (2009) 1038.
4. *Li H., Zhu Z., Li H., Li P., Zhou X.* // Journal of Colloid and Interface Science 349 (2010) 613.

5. *Ribeiro Nielson F.P., Mendes Fabiana M.T., Perez Carlos A.C., Souza Mariana M.V.M., Martin S.* // Appl. Catal. A: Gen. 347 (2008) 62.
6. *Navarro R., Pawelec B., Fierro J.L.G., Vasudevan P.T., Cambra J.F., Guemez M.B., Arias P.L.* // Fuel Processing Technology 61 (1999) 73.
7. *Shu Y., Ichikawa M.* // Catal. Today 71 (2001) 55.
8. *Chmielarz L., Kusrtrowski P., Michalik M., Dudek B., Piwowarska Z., Dziembaj R.* // Catal. Today 137 (2008) 242.
9. *Kalpesh B.S., Hasmukh A.P., Parimal A.P., Bahadur P., Bajaj H.C., Jasra R.V.* // Applied Clay Science 42 (2009) 386.
10. *Maki-Arvela P., Hajek J., Salmi T., Yu M.D.* // Appl. Catal. A. 292 (2005) 1.
11. *Singh U.K., Vannice M.A.* // Appl. Catal. A. 213 (2001) 1.
12. *Rolison D.R.* Nanomaterials: Synthesis, properties and application. Edelstein A.S., Cammarata R.C. (Eds.). Institute of Physics Publishing, Bristol (1996).
13. *Malyala R.V., Rode C.V., Arai M., Hegde S.G., Chaudhari R.V.* // Appl. Catal. A, 193, 1–2 (2000) 71.
14. Melendrez R., A. Alarcon Angel G.D., R. Gomez React. Kinet. // Catal. Lett. 2000, 70, 1, 113.
15. *Hajek J., Kumar N., Maki-Arvela P., Salmi T., Murzin D.Y., Paseka I., Heikkila T., Laine E., Laukkanen P., Vayrynen J.* // Appl. Catal. A, 251, 2 (2003) 385.
16. *Lashdaf M., Tiitta M., Venalainen T., Sterholm H.O., Krause A.O.I.* // Catal. Lett. 94, 1—2, (2004) 7.
17. *Chatterjee M., Iwasaki T., Onodera Y., Nagase T.* // Catal. Lett. 61, 3—4 (1999) 199.
18. *Chatterjee M., Ikushima Y., Zhao F.Y.* // Catal. Lett., 82, 1—2, (2002) 141.
19. *Chatterjee M., Iwasaki T., Onodera Y., Hayashi H., Ikushima Y., Nasage T., Ebina T.* // Appl. Clay Sci., 25, 3—4 (2004) 195.
20. *Szollosi G., Torok B., Baranyi L., Bartok M.* // J. Catal. 179, 2 (1998) 619.
21. *Reyes P., Rojas H., Pecchi G., Fierro J.L.G.* // J. Mol. Catal. A: Chem. 179, 1—2 (2002) 293.
22. *Sivakumar T., Mori T., Kubo J., Morikawa Y.* // Chem. Lett. 30, 9 (2001) 860.
23. *Sivakumar T., Krithiga T., Shanthi K., Mori T., Kubo J., Morikawa Y.* // J. Mol. Catal. A., 223, 1—2 (2004) 185.
24. *Bachiller-Baeza B., Rodriguez I., Guerrero-Ruiz A.* // Appl. Catal. A, 205, 1—2 (2001) 227.
25. *Consonni M., Jokic D., Murzin D.Y., Touroude R.J.* // J. Catal. 188, 1 (1999) 165.
26. *Milone C., Tropeano M.L., Gulino G., Neri G., Ingoglia R., Galvagno S.* // Chem. Commun. 8 (2002) 868.
27. *Okumura M., Akita T., Haruta M.* // Catal. Today, 74, 3—4 (2002) 265.
28. *Silva A.M., Santos O.A.A., Mendes M.J., Jordao E., Fraga M.A.* // Appl. Catal. A 241, 1—2 (2003) 155.
29. *Kijenski J., Winiarek P., Paryjczak T., Lewicki A., Mikołajska A.* // Appl. Catal. A, 233, 1—2 (2002) 171.
30. *Recchia S., Rossi C., Poli N., Fusi A., Sordelli L., Psaro R.* // J. Catal. 184, 1, (1999) 1.
31. *Klabunde K.J., Mulukutta R.S.* Nanoscale materials in chemistry. 2001. Ed. By Klabunde K.J., John Wiley & Sons, Inc., New York, p. 223.
32. *Mohr C., Claus P.* // Sci. Progress, 84, 4 (2001) 311.
33. *Bauer K., Garbe D.* Common fragrance and flavour materials. 1985. VCH, Weinheim.
34. *Gallezot P., Fendler G., Richard D.* // Catalysis of organic reactions. 1991. Pascoe W. (Ed.,), Marcel Dekker, New York, p. 1.
35. *Bartok M., Molnar A.* The chemistry of double bonded functional groups, Supplement A3, 1997, Patai S., Ed., Wiley, New York, p. 843.
36. *Coq B., Figueras F.* // Coord. Chem. Rev., 178—180, 2 (1998) 1753.
37. *Smith G.V., Notheisz F.* Heterogeneous catalysis in organic chemistry. 1999. Academic Press, London, p. 58.
38. *Lashdaf M., Krause A.O.I., Lindblad M., Tiitta M., Venalainen T.* // Appl. Catal. A, 241, 1—2 (2003) 65.
39. *Ryndin Y.A., Santini C.C., Prat D., Basset J.M.* // J. Catal. 190, 1—2 (2000) 364.
40. *Toshima N., Takahashi T.* // Bulletin Chemical Society of Japan, 65 (1992) 400.
41. *Kiraly Z., Veisz B., Mastalir A., Razga Z., Dekany I.* // Chem. Commun. (1999) 1925.
42. *Kiraly Z., Veisz B., Mastalir A., Kofarago G.* Langmuir, 17 (2001) 5381.
43. *Duff D.G., Edwards P.P., Johnson B.F.G.* // Journal Physical Chemistry, 99, 43, (1995) 15934.
44. *Hahakura S., Isoda S., Ogawa T., Moriguchi S., Kobayashi T.J.* // Cryst. Growth, 237–239, 3 (2002) 1942.
45. *Abid M.R., Touroude R.* // Catal. Lett. 69, 3—4 (2000) 139.
46. *Englisch M., Jentys A., Lercher J.A.* // J. Catal. 166 (1997) 25.
47. *Giroir-Fendler A., Richard D., Gallezot P.* // Studies in Surface Science and catalysis, 41 (1988) 171.
48. *Satagopan V., Chandalia S.B.* // J. Chem. Technol. Biotechnol. 60, 1 (1994) 17.
49. *Zhang L., Winterbottom J.M., Boyes A.P., Raymahasay S.* // J. Chem. Technol. Biotechnol. 72, 3 (1998) 264.
50. *Von Arx M., Mallat T., Baiker A.J.* // J. Mol. Catal. A: Chem. 148, 1–2 (1999) 275.
51. *Singh U.K., Vannice M.A.* // J. Catal. 199 (2001) 73.
52. *Hajek J., Kumar N., Maki-Arvela P., Salmi T., Murzin D.Y.* // J. Mol. Catal. A: Chem. 217 (2004) 145.

УДК 544.47; 547.571

СИНТЕЗ МЕТАЛЛСОДЕРЖАЩИХ МОНТМОРИЛЛОНИТНЫХ КАТАЛИЗАТОРОВ ДЛЯ РЕАКЦИЙ СЕЛЕКТИВНОГО ДЕГИДРИРОВАНИЯ

© 2012 г. **Д. Маникандан**[1,3], **Р.В. Мангаларайя**[1], **С. Анантакумар**[2], **Т. Сивакумар**[3]

[1] Отделение материаловедения, Инженерный факультет, Университет г. Консепсьон, Чили

[2] Отделение полезных ископаемых и материаловедения, Национальный Институт междисциплинарных наук и технологий, г. Тривандрум, Индия

[3] Лаборатория катализа, Отделение химических технологий, Технологический колледж, Университет Анна, г. Ченнай, Индия

Предложен метод синтеза металлсодержащих монтмориллонитных катализаторов, позволяющий вводить металлы в межслоевое пространство минералов. Показано, что межслойное пространство монтмориллонитов может служить наноразмерным реактором для получения мелкодисперсных металлических частиц, исключая их агрегацию. Образование наноразмерных металлических частиц между пластинами монтмориллонитов можно использовать для синтеза стабильных, хорошо диспергированных металлических катализаторов. По сравнению с обычными пористыми и нанесенными катализаторами такие катализаторы в реакциях селективного гидрирования позволяют повысить селективность, уменьшить вероятность протекания побочных реакций конденсации и циклизации. Известно, что селективное гидрирование коричного альдегида до коричного спирта используется в парфюмерной и пищевой промышленности. Осуществить реакцию с максимальной селективностью и высокой степенью конверсии – трудная задача. На активность и селективность катализаторов влияют природа металла и носителя, метод синтеза, размер частиц металлических катализаторов, растворитель, температура реакции, давление водорода и т.д.

В данной статье рассматривается жидкофазное гидрирование коричного альдегида на платиновых и рутенийсодержащих смектит/гекторит катализаторах при различных температурах и давлениях водорода. Изучены влияние растворителя и время контакта на степень конверсии и селективность катализаторов. Сопоставлены активность вновь синтезированных металлсодержащих смектит/гекторит катализаторов и полученных пропиткой в реакции гидрирования коричного альдегида.

В синтезе металлических наночастиц золя использовано поверхностно-активное вещество (ПАВ). Платиновый и рутениевый нанозоль получали добавлением металлических прекурсов, таких, как гексаплатинохлористоводородная кислота или гексааминорутениевый хлорид, содержащие 1 и 2 мас.% платины или рутения, соответственно, в воду в присутствии цетилтриметиламмония бромида с перемешиванием в течение 2 ч. Критическая концентрация мицелл ПАВ – это минимальная концентрация, при которой мицеллы образуются в водном растворе и предотвращают агрегирование металлических частиц путем образования адсорбированного слоя на поверхности частиц и их стабилизации в диспергированном состоянии в растворе. Хорошо диспергированные частицы формируются только, когда концентрация ПАВ в 10 раз превышает критическую концентрацию мицелл (для катионных ПАВ это значение составляет 0,92 ммоль/л). Катионный ПАВ способствует также длительной стабильности металлического гидрозоля, так как вертикально ориентированный бислой адсорбируется на поверхности металлических наночастиц (электростатическая и пространственная стабилизация).

Затем прекурсор в мицелле доведен до металлического состояния добавлением по каплям водного раствора $NaBH_4$ (0,05 г в 10 мл дистиллированной воды) и перемешиванием в течение примерно 3 ч.

Полученный металлический нанозоль черного цвета был добавлен отдельно в водную суспензию соответствующей глины и оставлен при интенсивном перемешивании приблизительно на 24 ч. Реакция ионного обмена Na^+ в случае смектита и Li^+ в случае гекторита с цетилтриметиламмонием (CTA^+) привела к образованию органоглинистого комплекса с одновременным внедрением частиц Pt или Ru, соответственно, во внутреннее пространство глины (между пластинами). Образцы монтмориллонита с внедренными частицами металла (черного цвета) тщательно промывались этанолом и толуолом для удаления избытка поверхностно-активных веществ в растворе и высушивались на воздухе. Реакции между Na^+ и Li^+ в межслойном пространстве и CTA^+ в мицелле стимулировали внедрение активных наночастиц металла в межслойное пространство. Ионы CTA^+, участвующие в реакции ионного обмена с Na^+, способствуют гидрофобности поверхности глины.

Рентгенограммы подтверждают, что кристалличность глинистых минералов не изменилась после внедрения металлических наночастиц. Данные рентгеновской дифракции показывают, что «фуллерова земля» (смектит) набухает в большей степени (от 1,472 до 5,923 нм), чем гекторит (от 1,193 до 1,92 нм). ПЭМ микрофотографии пропитанных катализаторов и с внедренными между плоскостями частицами металла подтверждают четкое рассеивание Pt и Ru наночастиц. Было установлено, что диаметр частиц металла составляет от 1 до 25 нм для различных катализаторов. Термограмма монтмориллонита свидетельствует о двух стадиях потери веса, а именно при 90 °C вследствие потери адсорбированных молекул воды и в области 170–350 °C из-за разложения ионов ПАВ. Из этих данных можно косвенно судить о термической стабильности и диапазоне температур для проведения каталитической реакции с использованием металлических монтмориллонитных катализаторов.

Результаты, полученные в жидкой фазе гидрирования коричного альдегида на синтезированных катализаторах, указывают, что катализаторы могут быть использованы в качестве альтернативных для реакций гидрирования. Pt-CTA-MM 1 катализатор оказался лучшим в реакции гидрирования коричного альдегида, максимальная конверсия составила 60 % и селективность – 79 % по коричному спирту при комнатной температуре и давлении водорода 9 бар. Катализатор Pt-CTA-MM 2 показал более высокую степень конверсии, чем Pt-CTA-MM 1 , но его селективность была меньше, что обусловлено наличием крупных частиц. Увеличенная каталитическая активность Pt монтмориллонитных катализаторов с лучшей селективностью обусловлена большим *d*-орбитальным расширением платины по сравнению с Ru, бóльшими расстояниями между слоями и большей кислотностью «фуллеровой земли» по сравнению с гекторитом. Давление водорода 9 бар и температура реакции 30 °C является оптимальной для достижения высокой конверсии и селективности. Повышение температуры и давления увеличивает только конверсию. Селективность уменьшается с ростом температуры и не изменяется с увеличением давления. Изучение влияния растворителя в реакции с коричным альдегидом показывает, что полярный растворитель в большей степени повышает конверсию образца с максимальной селективностью. Исследование влияния времени контакта показало отсутствие периода торможения для всех катализаторов в изученной реакции. Сравнение каталитической активности вновь синтезированных Pt и Ru катализаторов с пропитанными Pt и Ru катализаторами показало, что первые более селективны в отношении основного продукта – коричного спирта. Пропитанные катализаторы имели бóльшую активность, но меньшую селективность.